ELECTRONIC SUPPLEMENTARY INFORMATION

Ammonium Monoethyloxalate (AmEtOx): a New Agent for the Conservation of Carbonate Stone Substrates

M. Carla Aragoni,[a] Laura Giacopetti,[a] Massimiliano Arca,[a,*] Gianfranco Carcangiu,[b] Stefano Columbu,[a] Domingo Gimeno,[e] Francesco Isaia,[a] Vito Lippolis,[a] Paola Meloni,[c,d] Antonia Navarro Ezquerra,[f] Enrico Podda,[a] Jordi Rius,[g] Oriol Vallcorba,[h] and Anna Pintus[a,*]

[a] *Università degli Studi di Cagliari, Dipartimento di Scienze Chimiche e Geologiche, S.S. 554 bivio per Sestu, 09042 Monserrato (Cagliari), Italy. E-mail: apintus@unica.it, marca@unica.it*
[b] *Consiglio Nazionale Delle Ricerche (CNR), Istituto di Scienze dell'Atmosfera e Del Clima (ISAC), UOS di Cagliari c/o Dipartimento di Fisica, Università Degli Studi di Cagliari, S.S. 554 bivio per Sestu, Monserrato (Cagliari), 09042, Italy*
[c] *Dipartimento di Ingegneria Meccanica, Chimica e dei Materiali, via Marengo 2, 09123, Cagliari, Italy*
[d] *Laboratorio Colle di Bonaria, Università degli Studi di Cagliari, Via Ravenna snc, Cagliari, 09125, Italy*
[e] *Facultat de Ciències de la Terra, Universitat de Barcelona, c/ Martí i Franquès s/n, 08028 Barcelona, Spain*
[f] *Departamento de Tecnología de la Arquitectura, EPSEB-UPC, Avda. Doctor Marañón, 44-50, 08028 Barcelona, Spain*
[g] *Institut de Ciència de Materials de Barcelona (CSIC), Campus de la UAB, 08193 Bellaterra, Spain*
[h] *ALBA Synchrotron Light Source – CELLS. 08290 Cerdanyola del Vallès, Barcelona, Spain*

Table S1. Penetration depth (mm) values and thickness of the protective layer (μm) for selected inorganic consolidants applied by immersion of stone samples in water solutions, and relative methods of determination.

Consolidant	Stone	Penetration depth	Thickness of protective layer	Method	Ref.
AmEtOx 5–12% w/w	Artificially weathered marble	0.2	30–50	tts-μXRD	This work
	Biomicritic limestone	0.8	200–500		
AmOx 2–5%	Marble	-	-	-	-
	Cretaceous Limestone	0.026-0.182	16–38	SR-μXRD	2
AmMeOx 5–12.3% w/w	Naturally weathered Carrara Marble	0.15[a]	10–15	SEM	3
	Biomicritic Limestone	-	40		
AmOxam 5–11.5% w/w	Naturally weathered Carrara Marble	0.4	30–50	SEM	3
	Biomicritic Limestone	1.0	70–100		
AmPhOxam 2.5%	Naturally weathered Carrara Marble	–	10–15	SEM	4
	Biomicritic Limestone	0.3	4		
DAP 40%	Artificially weathered Marble	5.0	1000	SEM-EDX	5
	Biomicritic Limestone	10.0	1500		

[a] Hydroalcoholic solution.

Table S2. Ultrasonic P-wave velocity Vp (km s^{-1}) measured in the three orthogonal planes, anisotropy indices dM and dm (%), MIP mean porosity P (%), average pore size radius r_{av} (μm), and apparent density ρ (g/cm^3), for Statuario Michelangelo marble (Carrara) before (a, unweathered) and after one (b) or two (c) thermal-shock accelerated weathering treatments.

	Vp (x)	Vp (y)	Vp (z)	Vp (x, y, z)	ΔVp (%)	dM (%)	dm (%)	P	ΔP (%)	r_{av}	Δ r_{av} (%)	ρ	$\Delta\rho$ (%)
a	5.52(1)	5.78(2)	5.81(3)	5.70	–	4.1	1.9	0.5(1)	–	0.16(2)	–	2.7(1)	–
b	1.51(8)	1.81(4)	1.65(7)	1.66	–71.0	13	8.9	–	–	–	–	–	–
c	1.42 (6)	1.63(2)	1.54(9)	1.53	–73.2	9.8	6.2	6.9(7)	1280	0.35(3)	119	2.5(1)	–4.1

Table S3. Selected experimental bond lengths (Å) and angles (°), and corresponding optimized parameters for the $EtOx^-$ anion in the gas phase and water (IEF-PCM SCRF model). Atom numbering scheme as in Figure 5.

	Structural data[a]	Gas	Water
C1–C2	1.540	1.542	1.534
C1–O1	1.232	1.240	1.244
C1–O2	1.271	1.239	1.243
C3–O3	1.207	1.208	1.210
C3–O4	1.335	1.364	1.336
O4–C3	1.456	1.418	1.439
C3–C4	1.504	1.514	1.509
O1–C1–O2	127.64	132.15	129.91
O3–C2–O4	123.96	121.40	123.95
O1–C1–C2–O4	2.54	88.19	84.56
C2–O4–C3–C4	176.56	86.15	88.04

[a] Taken from Ref. 1.

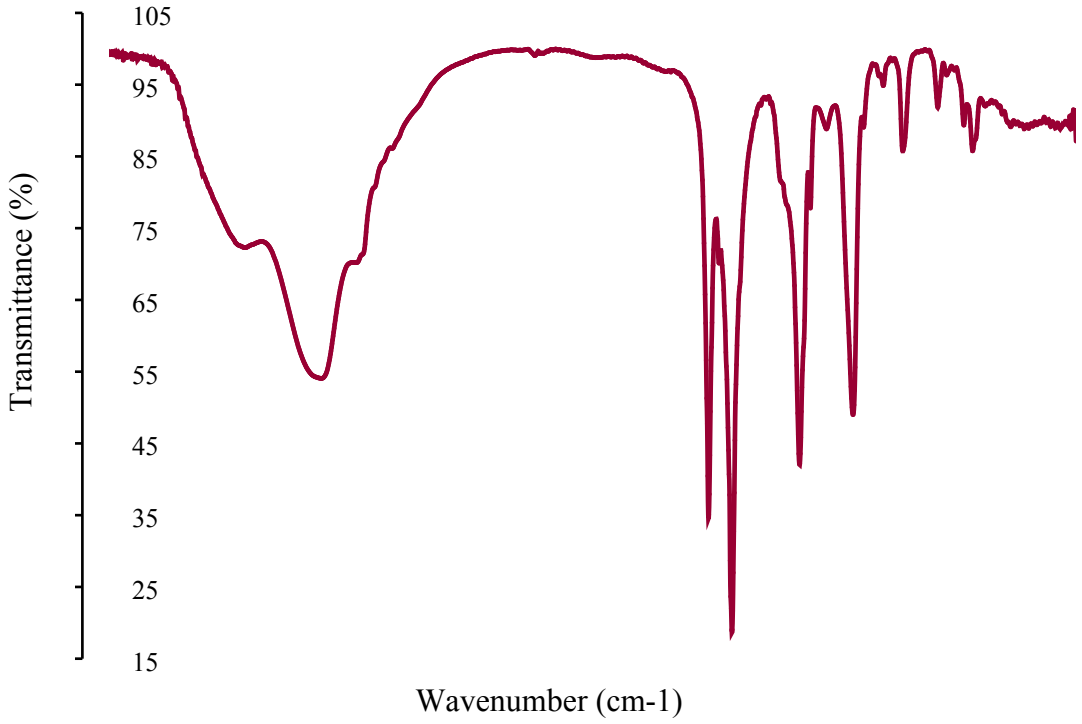

Figure S1. FT-IR spectrum of AmEtOx (KBr pellet).

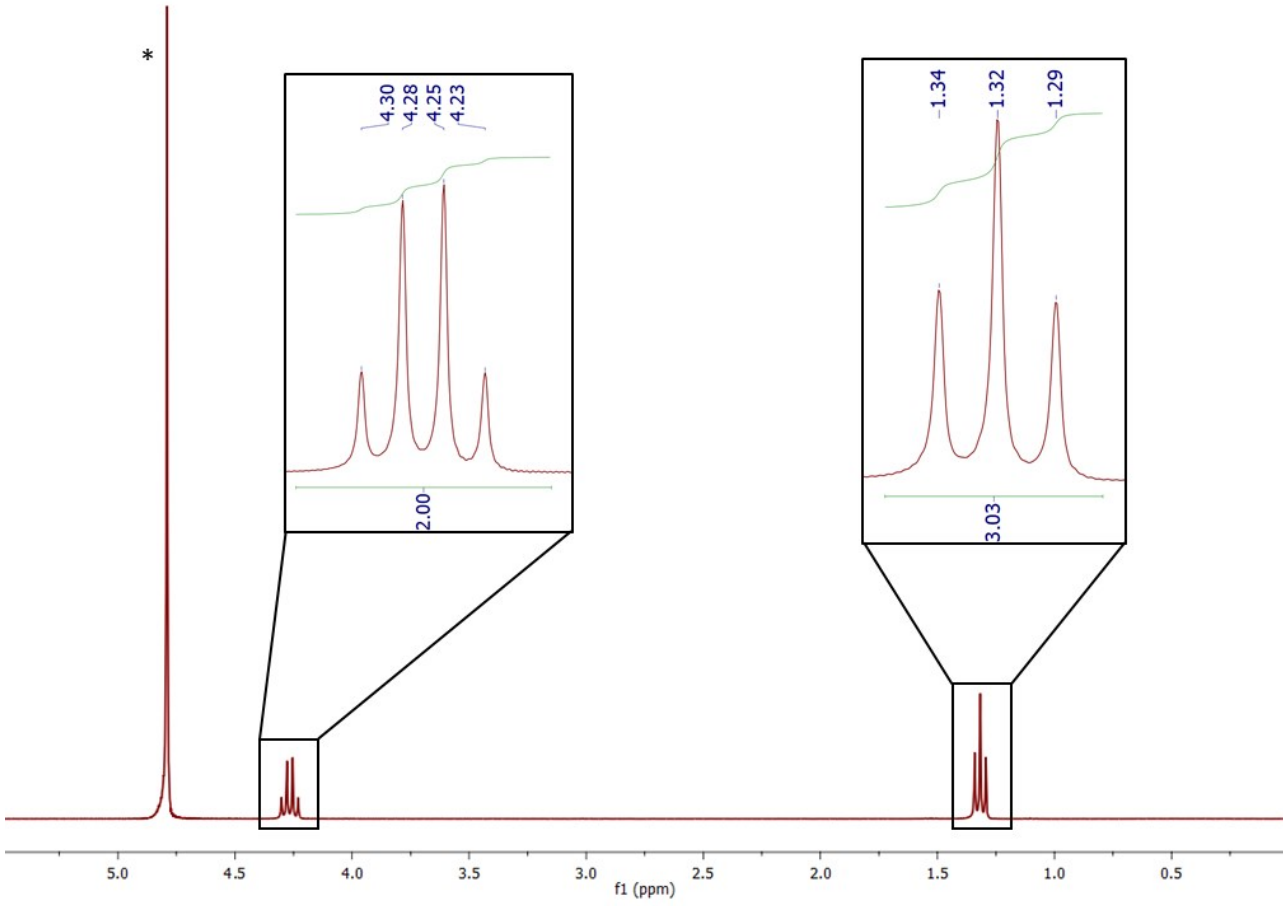

Figure S2. ^{1}H–NMR (D_2O, 300 MHz) spectrum of AmEtOx. The peak marked with an asterisk corresponds to the solvent residual signal.

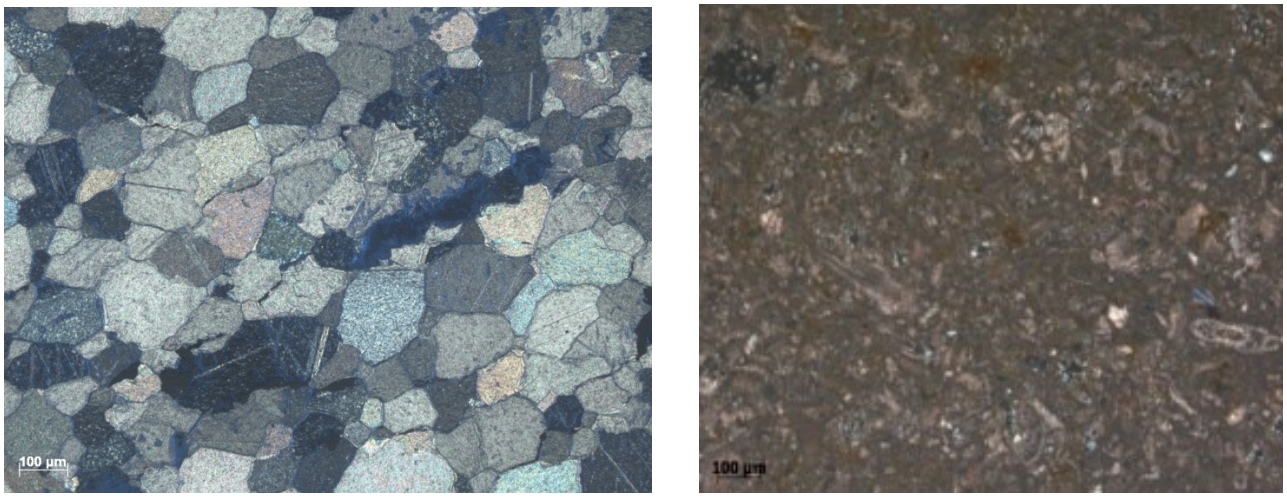

Figure S3. Thin sections photomicrographs (CTPL mode) of untreated Carrara marble (left) and biomicritic limestone (right) samples. Carrara marble shows a typical homeoblastic polygonal microstructure. The biomicritic limestone reveals an abundant microfossilifer fauna embedded within a micritic matrix. The carbonate cement is very scarce.

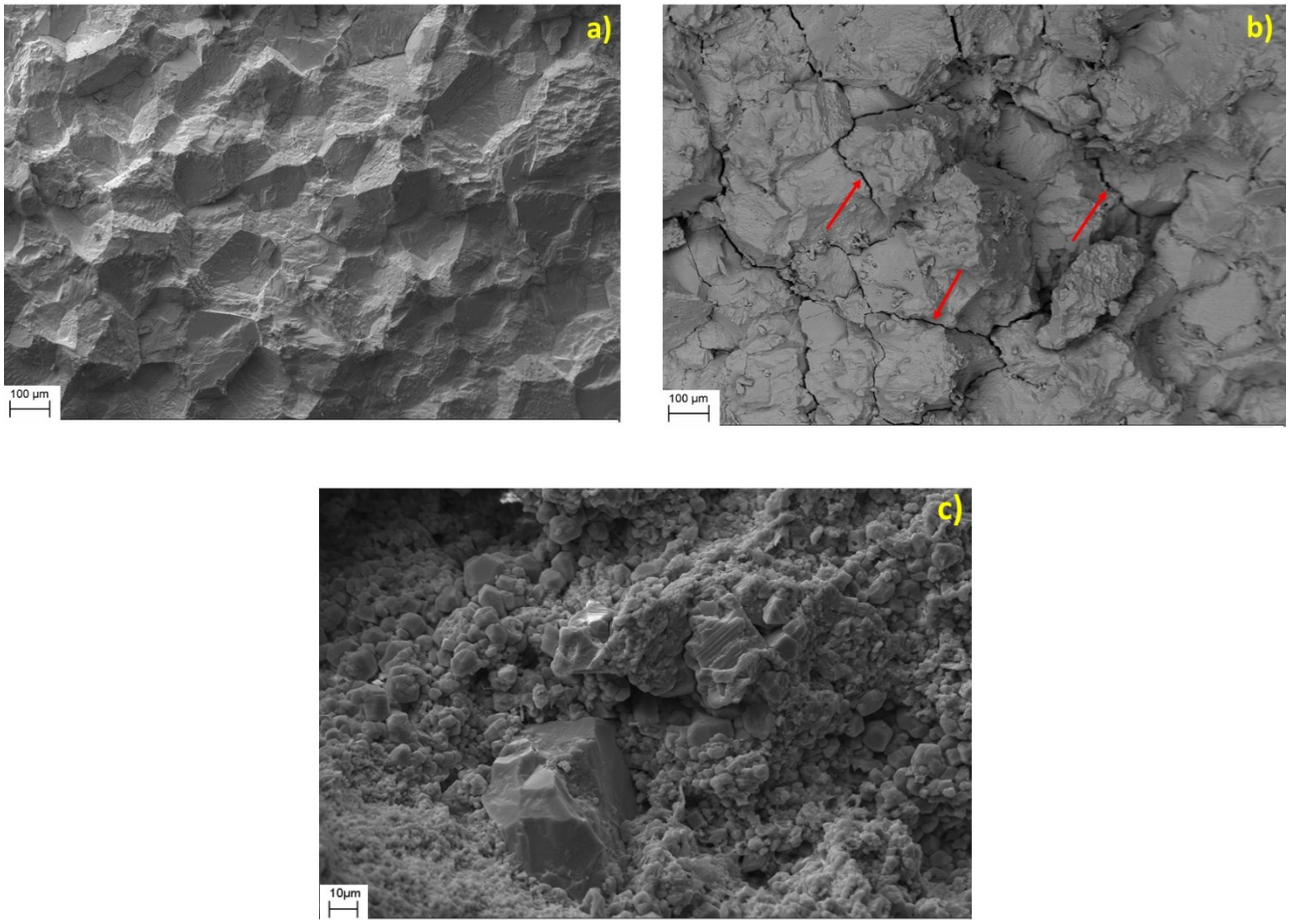

Figure S4. SEM images of untreated (a) and artificially weathered (b) Carrara marble samples, and untreated biomicritic limestone (c). The red arrows highlight some of the micro-cracks formed after the thermal treatment.

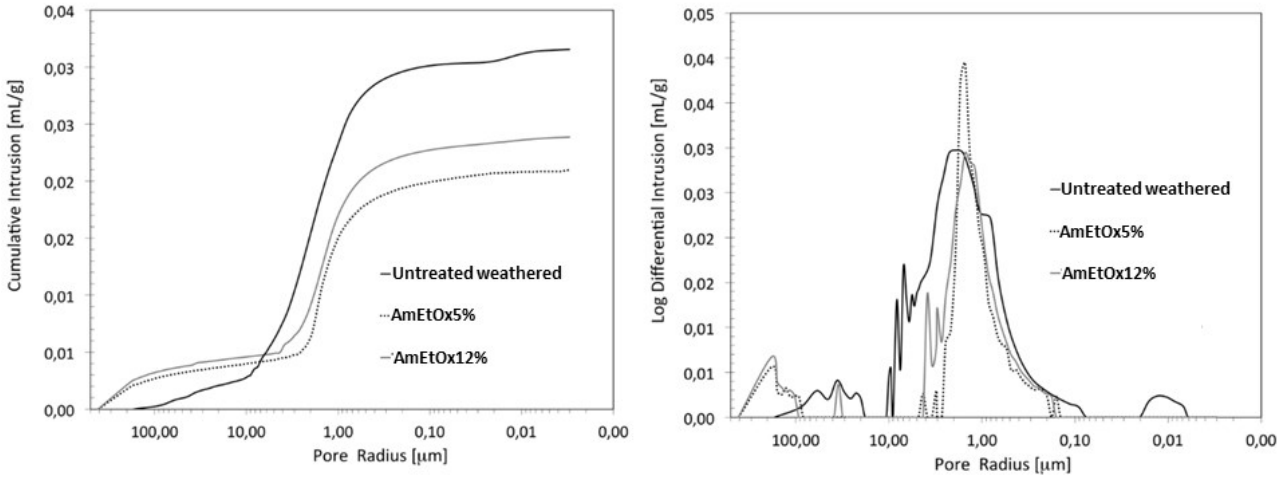

Figure S5. MIP cumulative (left) and Log differential (right) intrusion versus pore size radius for three selected thermally weathered Carrara marble samples before and after treatment with AmEtOx 5% and 12% w/w aqueous solutions.

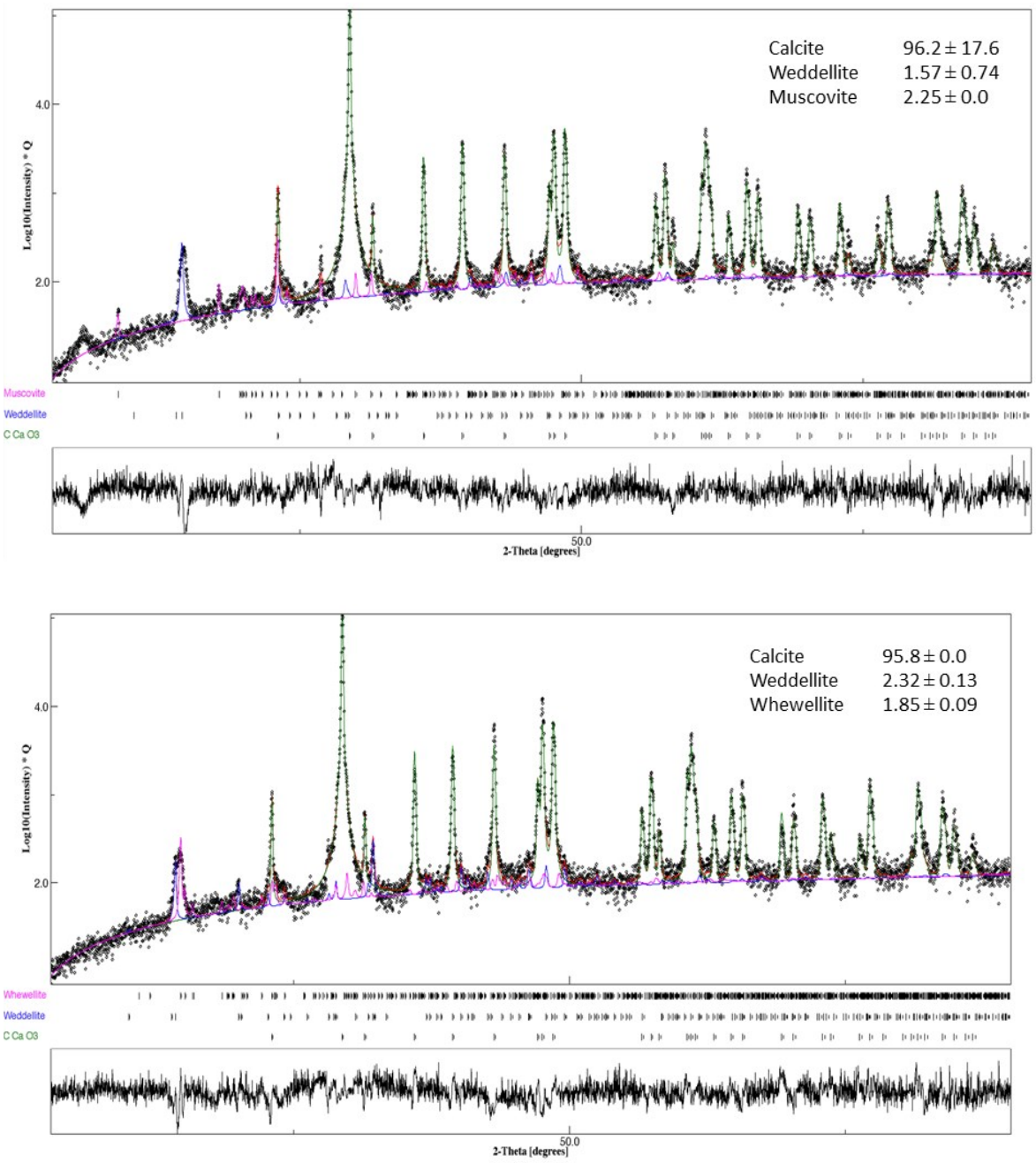

Figure S6. Quantitative XRD-analysis of powdered thermally weathered Carrara marble samples treated with AmEtOx 5% (top) and 12% w/w (bottom) aqueous solutions.

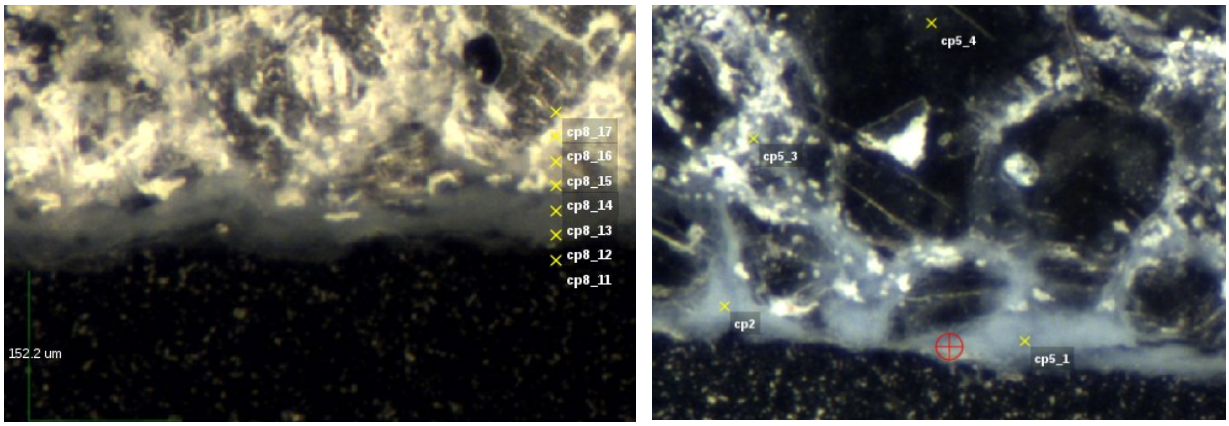

Figure S7. Photomicrographs of thin sections of thermally weathered Carrara marble samples treated with AmEtOx 5% (left) and 12% w/w (right) aqueous solutions, showing the points sampled by tts-μXRD.

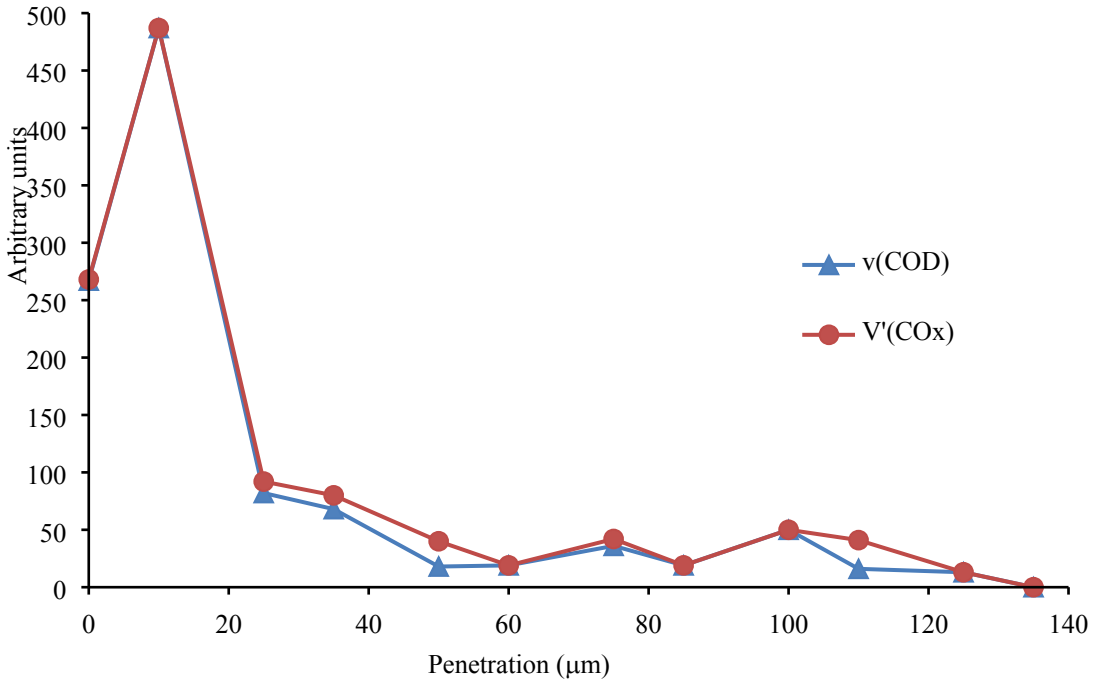

Figure S8. Evolution of hydrated calcium oxalates as a function of the penetration depth in a sample of thermally weathered Carrara marble after the treatment with an AmEtOx 5% w/w aqueous solution. v(COD) represents the (relative) volume fraction of weddellite, while V'(COx) is the total volume of diffracting calcium oxalate phases. Notice that for the sampling point at 0 µm, i.e. exactly at the end of the layer, only half of the incoming beam is diffracted which results in an apparent reduction of V' (COx).

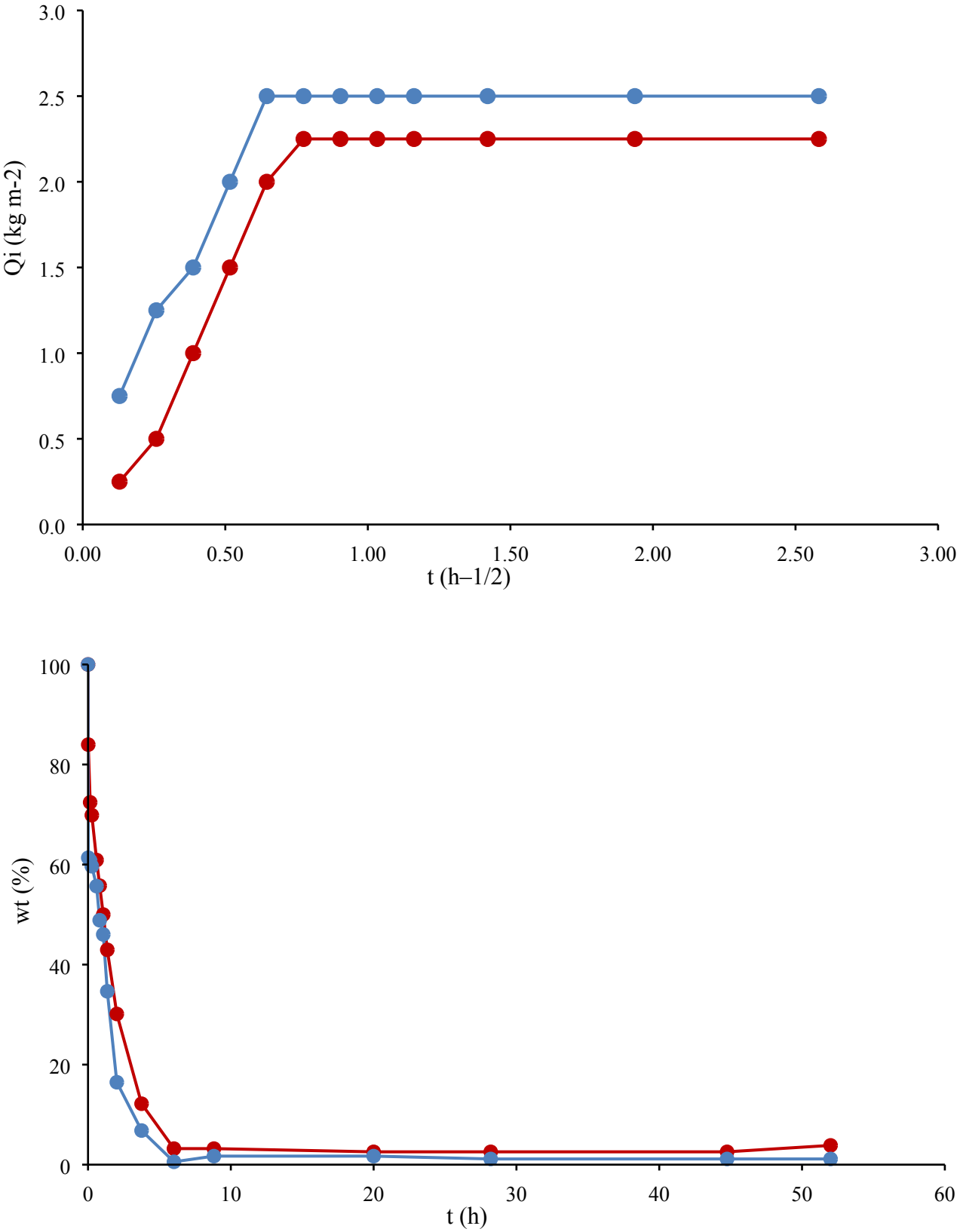

Figure S9. Water capillary absorption (top) and desorption (bottom) curves for thermally weathered Carrara marble samples before (blue) and after (red) the treatment with an AmEtOx 5.0% w/w aqueous solution.

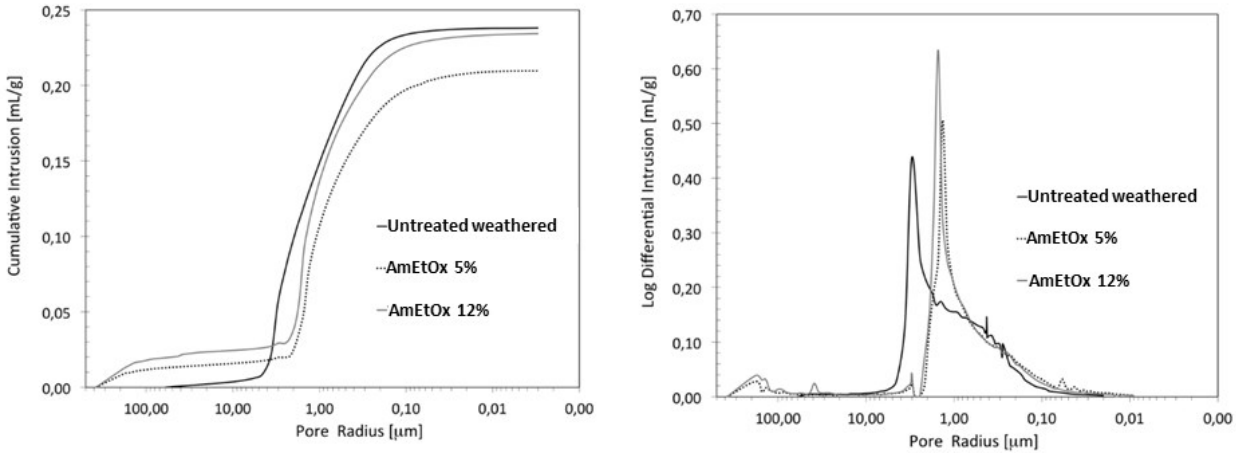

Figure S10. MIP cumulative (left) and Log differential (right) intrusion versus pore size radius for three selected biomicritic limestone samples before and after treatment with AmEtOx 5% and 12% w/w aqueous solutions.

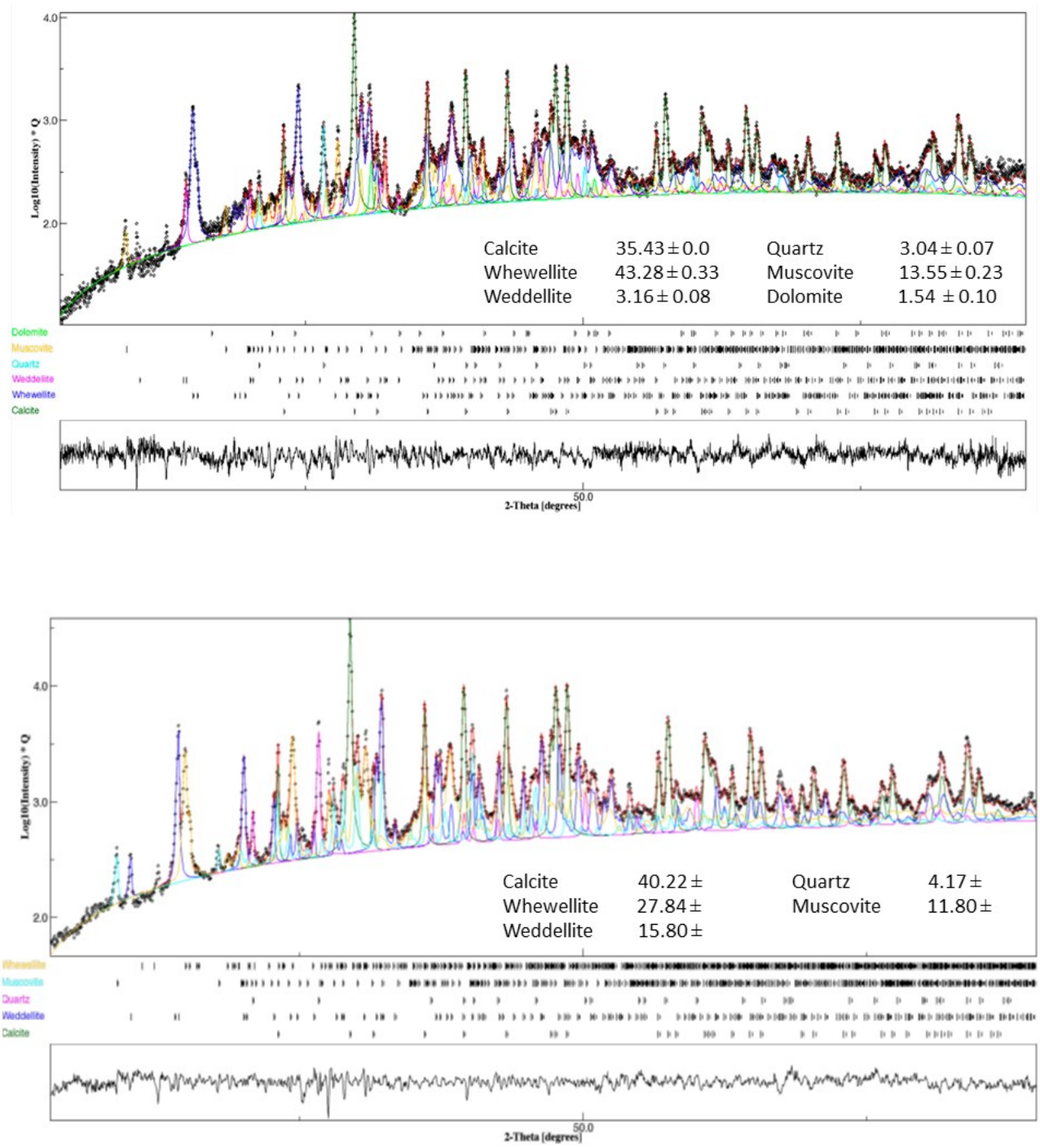

Figure S11. Quantitative XRD-analysis of powdered biomicritic limestone samples treated with AmEtOx 5% (top) and 12% w/w (bottom) aqueous solutions.

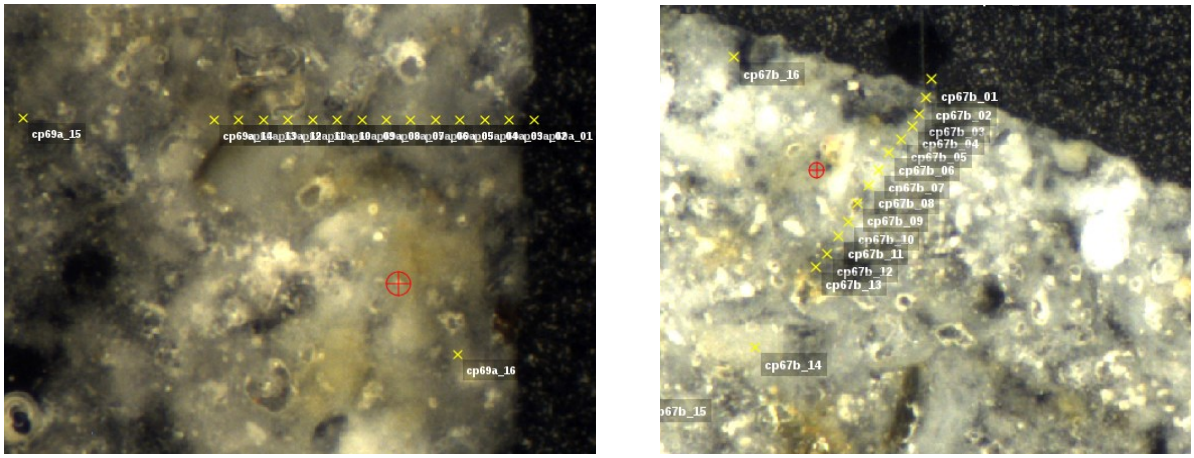

Figure S12. Photomicrographs of thin sections of biomicritic limestone samples treated with AmEtOx 5% (left, sampling line a) and 12.0% w/w (right, line b) aqueous solutions, showing part of the measured points.

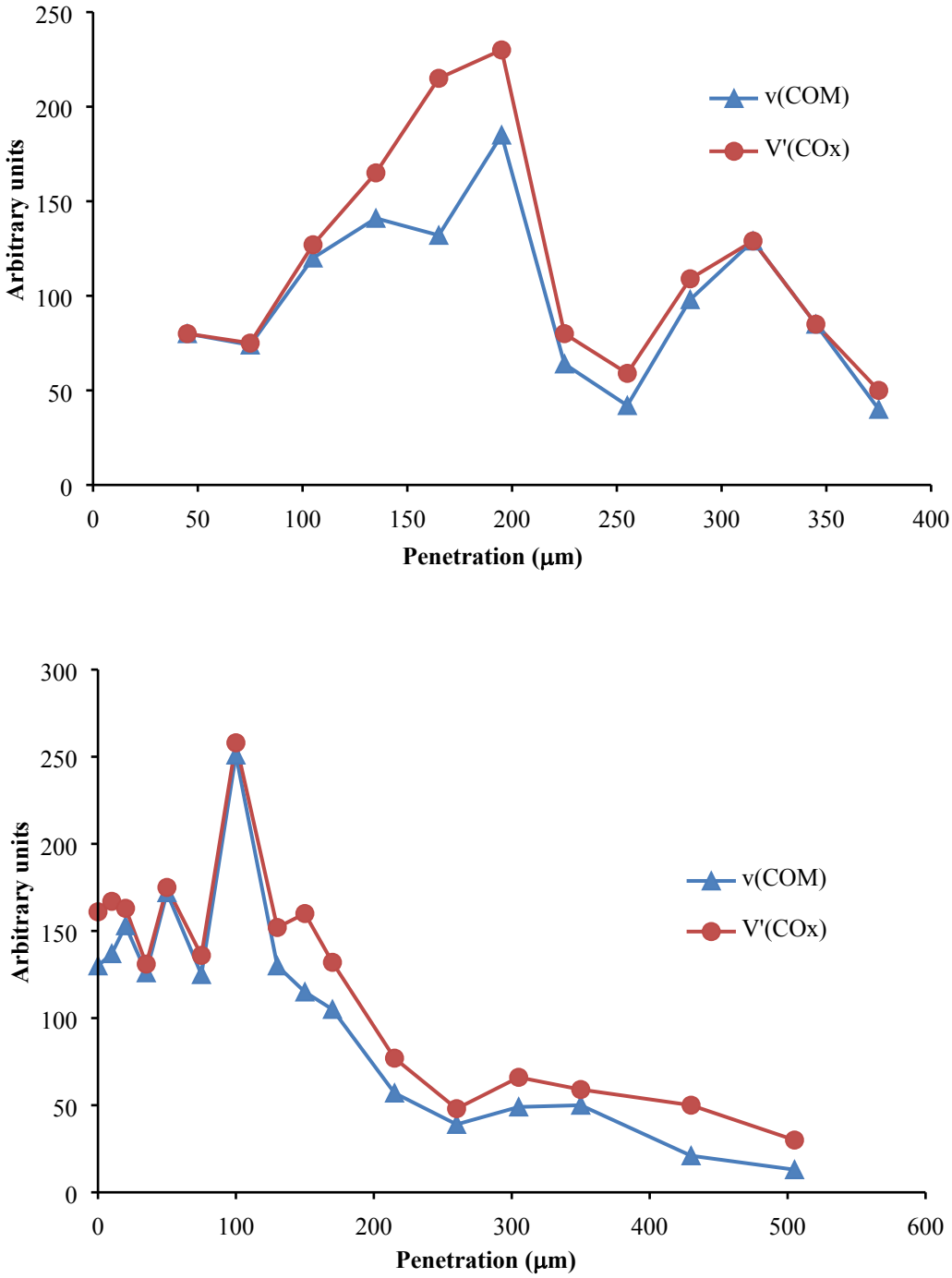

Figure S13. Plots showing, as a function of the penetration, the evolution of the whewellite fraction v(COM) in the total diffracting volume of calcium oxalates V'(COx) for a biomicritic limestone sample treated with an AmEtOx 5% w/w aqueous solution (top: sampling line a with 12 points; bottom: line b with 16 points). The penetration refers to the shortest distance from the target point to the surface.

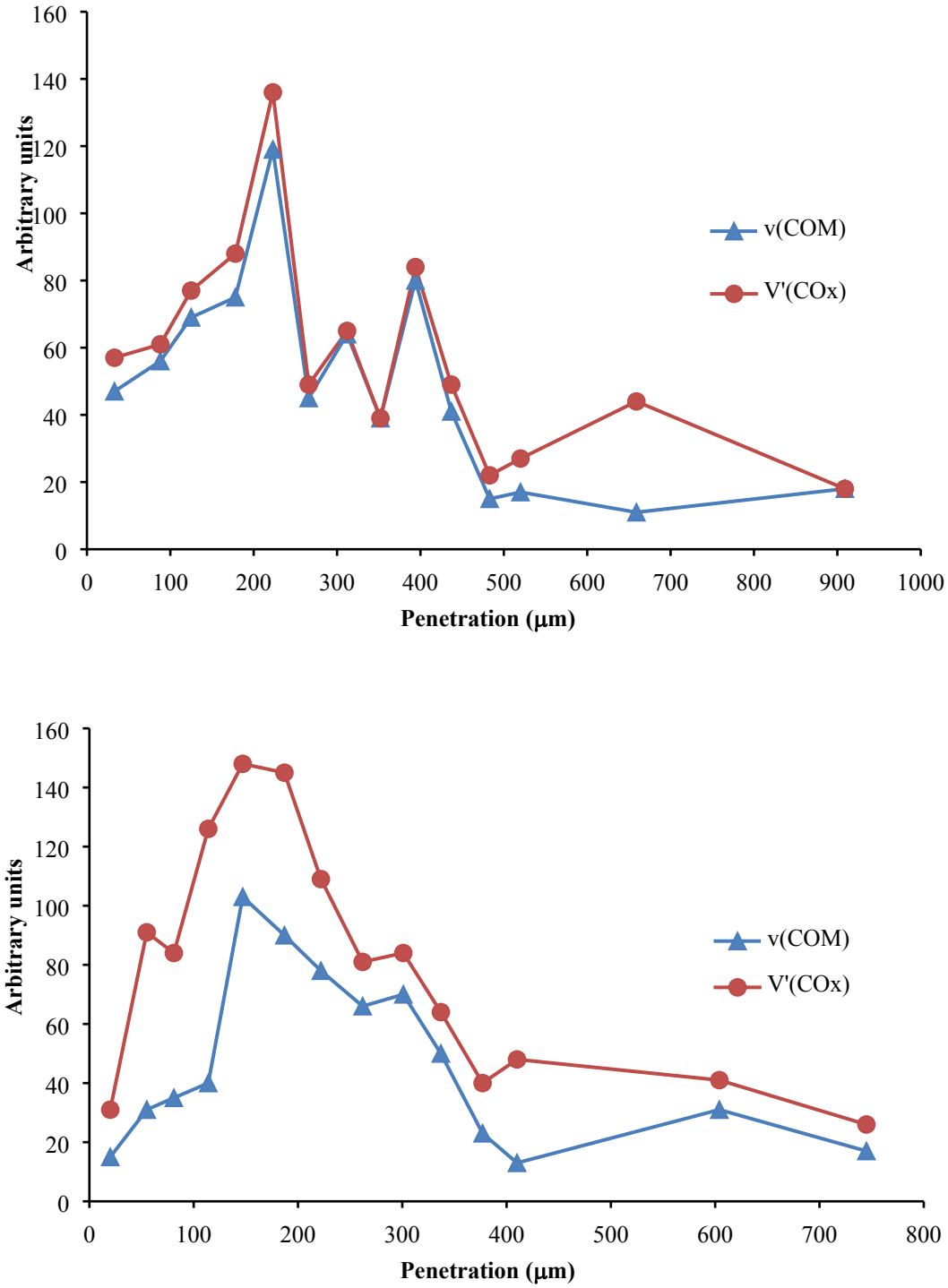

Figure S14. Plots showing, as a function of the penetration, the evolution of the whewellite fraction v(COM) in the total diffracting volume of calcium oxalates V'(COx) for a biomicritic limestone sample treated with an AmEtOx 12% w/w aqueous solution (top: sampling line a; bottom: line b). The penetration refers to the shortest distance from the target point to the surface.

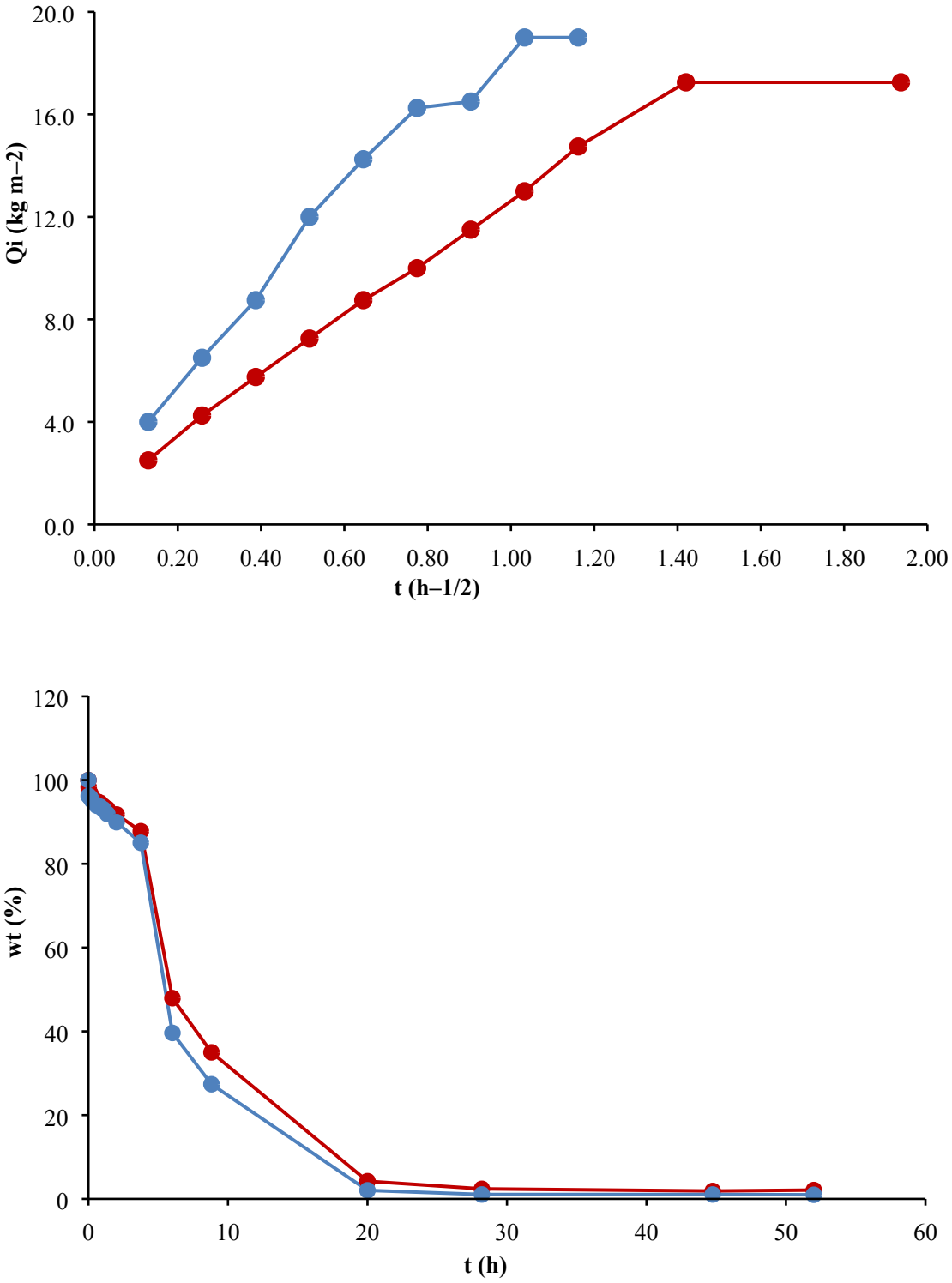

Figure S15. Water capillary absorption (top) and desorption (bottom) curves for biomicritic limestone samples before (blue) and after (red) the treatment with an AmEtOx 5% w/w aqueous solution.

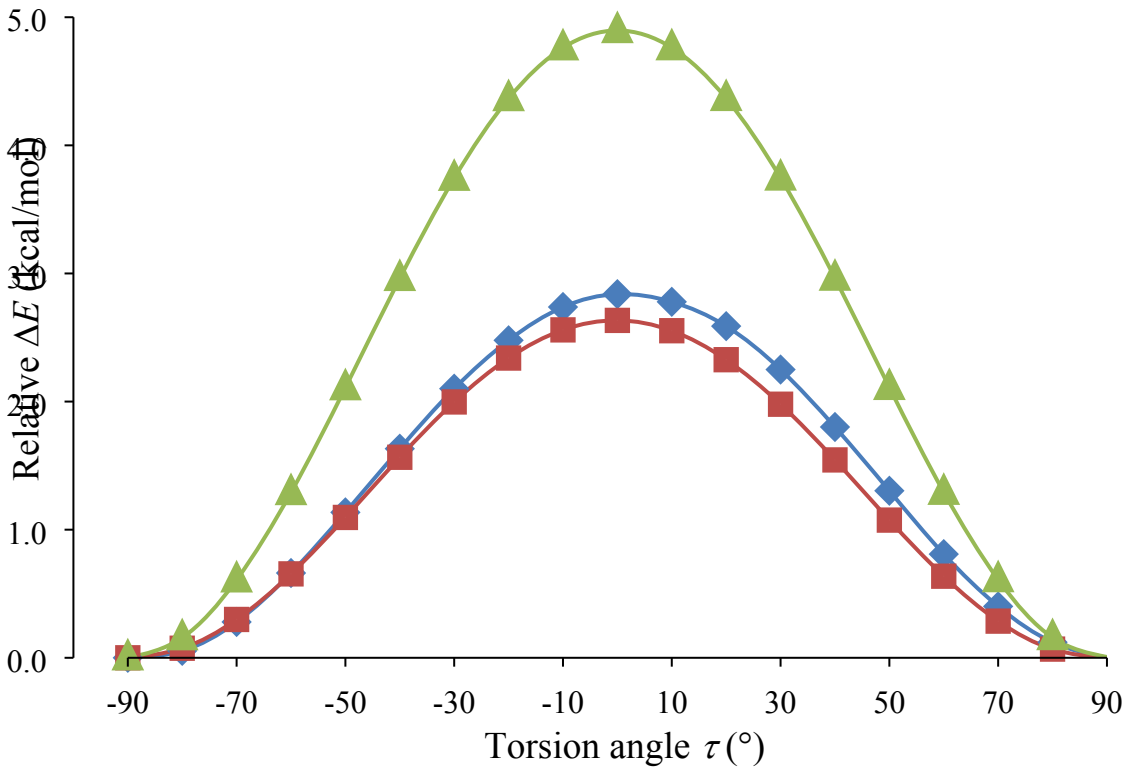

Figure S16. Relative energy variation ΔE of the total electronic energy as a function of torsion angle τ (O1–C1–C2–O3 dihedral; atom labelling scheme as in Figure 5) calculated for Ox^{2-} (triangles), $MeOx^{-}$ (squares), and $EtOx^{-}$ (rhombs) anions at the DFT level in the gas phase.

REFERENCES

(1) Deng, X.; Liang, J. T.; Peterson, M.; Rynberg, R.; Cheung, E.; Mani, N. S. *J. Org. Chem.* **2010**, *75* (6), 1940–1947.

(2) Mudronja, D.; Vanmeert, F.; Hellemans, K.; Fazinic, S.; Janssens, K.; Tibljas, D.; Rogosic, M.; Jakovljevic, S. *Appl. Phys. A Mater. Sci. Process.* **2013**, *111* (1), 109–119.

(3) Maiore, L.; Aragoni, M. C.; Carcangiu, G.; Cocco, O.; Isaia, F.; Lippolis, V.; Meloni, P.; Murru, A.; Tuveri, E.; Arca, M. *J. Colloid Interface Sci.* **2015**, *448*, 320–330.

(4) Maiore, L.; Aragoni, M. C.; Carcangiu, G.; Cocco, O.; Isaia, F.; Lippolis, V.; Meloni, P.; Murru, A.; Slawin, A. M. Z.; Tuveri, E.; Woollins, J. D.; Arca, M. *New J. Chem.* **2016**, *40* (3), 2768–2774.

(5) Murru, A.; Fort, R. *J. Cult. Herit.* **2019**, 42, 45–55.